# Electrometry on charge traps with a single-electron transistor

Miha Furlan*
*Solid State Physics Laboratory, ETH Zürich, CH-8093 Zürich, Switzerland and*
*Swiss Federal Office of Metrology and Accreditation METAS, CH-3003 Bern-Wabern, Switzerland*

Sergey V. Lotkhov
*Physikalisch-Technische Bundesanstalt PTB, D-38116 Braunschweig, Germany*
(Received 23 September 2002; published 16 May 2003)

Background charge fluctuators are studied individually by means of a single-electron transistor with multiple independent gates. Operation of the device in a feedback mode allows electrometric sensing of the charged background and its behavior upon electric potential variations due to geometrically different gates. Pulse height spectra and the hysteresis of charge trapping transitions are discussed as specific signatures of distinct fluctuators. The location of individual traps is determined from the experimental data and based on electrostatic calculations.

DOI: 10.1103/PhysRevB.67.205313 PACS number(s): 73.23.Hk, 71.55.−i, 72.20.Jv

## I. INTRODUCTION

Single-electron charging effects are among the most celebrated phenomena of mesoscopic physics. A very serious problem of mesoscopic electronic devices (and an extension of their high sensitivity) is fluctuating background charge. In spite of increased efforts in fabrication technology to produce high purity components, imperfections in solid state devices leading to interface or bulk trap states are responsible for background charge fluctuations. The significance of this problem is well known e.g., by the metal oxide semiconductor field effect transistor community,[1] but it is at least as crucial for potentially useful nanodevice applications.

The metallic single–electron transistor (SET) (Refs. 2 and 3) is one of the simplest and most extensively studied architectures manifesting Coulomb blockade. Due to its extreme charge sensitivity and the ability to transfer individual electrons, SETs have been proposed for a variety of applications or as building blocks of future electronics. It is known, however, that device sensitivity at dc operation is limited by low frequency input noise due to dynamic charge fluctuations in the vicinity of the SET, in metallic[4,5] as well as in semiconductor[6,7] devices. A possible solution to this problem is provided, e.g., by the radio frequency SET[8] operating well above the $1/f$ noise spectrum, or by appropriate device fabrication aiming for optimal shielding of the SET island against external charge perturbations.[9]

At least as serious as the dynamic noise is the static offset charge problem, which sets the device in an initial random state due to the random configuration of the quasistatic charge background. Fluctuators with large time constants but strong electrostatic influence on the device characteristics may shift the operation point such that repeated tuning of the biasing condition is required. This disadvantageous though not unusual scenario severely reduces the reliability of SETs for broader applications. Furthermore, it has also been suggested that photon assisted tunneling (PAT) due to background charge fluctuations as extrapolated from $1/f$ noise spectra may be the accuracy limiting process in high precision experiments.[10]

From a different perspective, charging effects in ultrasmall electronic devices may serve as the base mechanism of memory devices.[11] Due to technological limitations, operation of lithographically prepared single–electron devices is restricted to very low temperatures. However, the small size of charge traps (on the order of 1 nm) due to intrinsic impurities potentially allows manipulation of single charges at room temperature. If the random nature of impurities can be controlled or at least their behavior selectively discriminated, the discrete charging of traps can provide the essential process in high-density nonvolatile memory devices.

Therefore, due to the crucial role of background charge fluctuations for mesoscopic devices (as well as for microelectronics in general), a profound understanding of charge trapping processes is most desirable. We have performed extensive experimental studies on charge fluctuations in the vicinity of a multiple gate SET (see Fig. 1). We are able to identify the location and electronic configuration of individual metastable trap states. Our method provides a tool for characterizing the charge background and for optimizing the operation point with a working device with respect to noise performance, i.e., the mesoscopic sample under investigation and the detector for charge fluctuations are the same.

## II. EXPERIMENT

Experimental sensing of environmental charges is the main focus of this paper. Because the results certainly depend on the device topology and the substrate and lithographic quality, a detailed knowledge of the device fabrication is essential and its description is given in the following part. The experimental setup and the measurement procedure, which allow a virtually continuous resolution of charge fluctuations as a function of gate potentials, follow in the second part of this section. The third part presents the results.

### A. Device fabrication

The structure of type $Al/AlO_x/Al$ was fabricated by the two angle evaporation technique[12] on a thermally oxidized

 

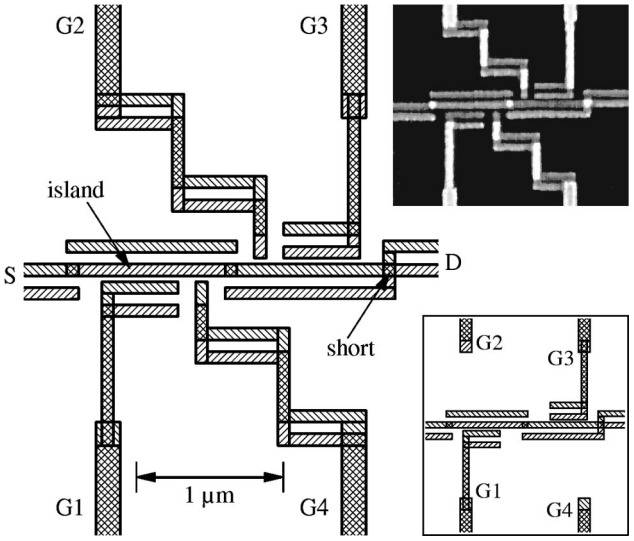


FIG. 1. Layout of the multigate SET (on the left) showing the actual metal depositions from the two angle evaporation (note the different hatching). The island closer to the source (S) couples to the electrodes via small high resistance tunnel junctions, whereas the other ''island'' of the original electron pump design has a lithographically defined short to drain (D). The AFM picture (inset top right) shows the overlap regions (brighter is higher) of the same device (type A). The alternative device (type B) differs only by more distant gates G2 and G4 (inset bottom right). The narrow strip lines have a width of 80 nm.

(300 nm deep) wafer of monocrystal Si. The trilayer mask *PMMA*/Ge/*PMMA-MAA* (Copolymer), 100, 30, and 300 nm thick, respectively (top to bottom), was exposed in the e-beam pattern generator Philips EBPG 4, both in the part of the fine structure and in the part of the contact leads and pads. After development of the PMMA in the mixture of MIBK/IPA, 1:2, for 1 min, the pattern was transferred to the layer of Ge by means of reactive-sputter etching ($CF_4$, 1 Pa, rf-power density 0.2 W/cm$^2$, 75 s), and then through the layer of the Copolymer ($O_2$, 0.8 Pa, 0.1 W/cm$^2$, 3 min) down to the substrate oxide with sufficient overetch time, which was necessary to compensate for the process nonuniformities. The undercut space necessary for oblique deposition was formed by isotropic etching of Copolymer at high oxygen pressure (30 Pa, 0.1 W/cm$^2$, 20 min). At this stage the surface oxide of the substrate was exposed to the oxygen plasma, which we believe might have helped in restoring the oxide quality after the previous sputter-etch step. The metal structure was deposited by the *e*-beam evaporator in one vacuum run and was formed by two conform layers of Al (25 and 35 nm thick) evaporated at 0.3 nm/s at the angles of $+14°$ and $-14°$, respectively. The base pressure in the evaporation chamber was below $10^{-5}$ Pa. The junctions ($80\times80$ nm$^2$ in size) were formed as the overlapped tips of the Al microstrips belonging to different layers. The dielectric barrier was formed by room temperature oxidation of the first Al layer (10 min at pure oxygen of 1 mbar) before the deposition of the second layer. After evaporation the sample was immersed in acetone for mask liftoff.

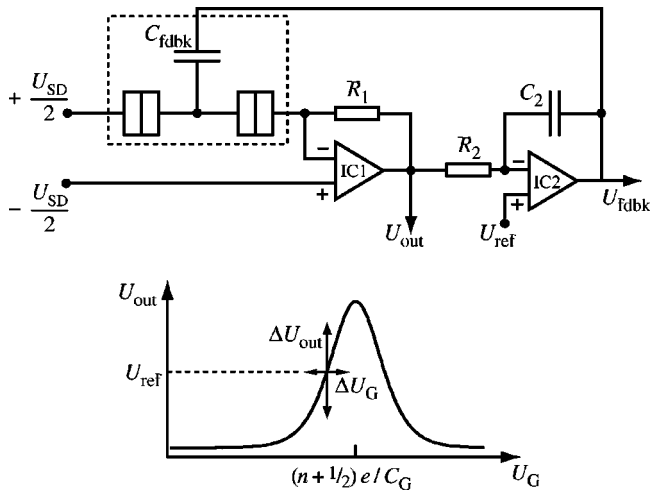


FIG. 2. Schematic readout circuit with voltage biased SET (dashed rectangle at low temperature), transimpedance amplifier (IC1) and feedback circuitry (IC2). The signal attenuators and filters used are omitted here for clarity. A measured Coulomb blockade peak (nonzero conductance around $(n+1/2)e$ island charge) is shown in the lower part, illustrating the effect of a potential variation $\Delta U_G$.

The only unknown or uncontrollable process influencing the physical properties of the samples is the long-term oxidation when stocking them. In spite of the high-quality fabrication and proven long-term stability of the devices, very slow oxide formation at the interfaces inevitably continues, which may, eventually together with ion diffusion, subsequently introduce shallow defects.

### B. Experimental setup and measurement procedure

Measurements were performed in a dilution cryostat with a base temperature of 5 mK, whereas the effective electron temperature of our system was found[13] to be 45 mK. The lines running from the room temperature electronics to the cold SET devices were filtered against microwave propagation with 2 m Thermocoax cables[14] each, and the sample holder was thoroughly enclosed to be electromagnetically tight. A magnetic field of typically 1 T was applied to suppress superconductivity of the aluminum devices.

The bias and readout electronics is schematically drawn in Fig. 2. It consists of a symmetrically voltage driven SET, where the current $I_{SET}$ through the transistor is sensed by the transimpedance amplifier IC1 (with feedback resistor $R_1 \gg R_{SET}$, where $R_{SET}$ is the asymptotic SET device series resistance). The input impedance of IC1 is required to be very high, then the current through the SET is given by

$$I_{SET} = -\frac{2U_{out}+U_{SD}}{2R_1}, \tag{1}$$

where $U_{SD}$ is the source-drain voltage.

The measurements discussed here were performed with a feedback circuitry holding the SET island at constant potential (or charge) irrespective of external potential variations. This was achieved by biasing the device at a Coulomb block-

ade peak at high gain $\eta = dU_{out}/dU_G$ (see the lower part of Fig. 2), integrating $U_{out}$ (right hand part of circuit with IC2 in Fig. 2) and feeding the signal back to $G_{fdbk}$, the feedback gate. When $U_{out}$ changes by $\Delta U_{out}$ for whatever reason, the feedback circuit reacts with a voltage $\Delta U_{fdbk} = -\Delta U_{out}/\eta$ in order to adjust $U_{out}$ to $U_{ref}$ (the minus sign stems from the inverting integrator circuit). In general, the requirement for the island to stay on constant potential is

$$\sum q_i = \sum U_i C_i = \text{const}, \tag{2}$$

where $q_i$ is the charge influenced on the island by the $i$th gate with capacitance $C_i$ being at the potential $U_i$. Therefore, upon a variation $\Delta U_i$ the influenced charge is modulated (i.e., the gate modulation curve is shifted by $-\Delta q_i/C_i$) and the feedback circuit response, still without background charges, is a voltage

$$\Delta U_{fdbk} = -\Delta U_i \frac{C_i}{C_{fdbk}} \tag{3}$$

to the feedback gate with capacitance $C_{fdbk}$. If the device is an isolated system where the only non-zero potentials are supplied by the gates, the feedback voltage is always linear to the gate voltages, see Eq. (3), and can be subtracted in the data analysis of gate sweep measurements. However, if extra background charges in the vicinity of the SET are taken into account, they modify the island potential such that

$$\delta Q_{island} = -\Delta U_{fdbk} C_{fdbk} \tag{4}$$

is the corresponding charge shift which is compensated for by $G_{fdbk}$.

The dynamics of our electronics are limited to low frequencies. The main constraint on the response is given by the $RC$ time of the SET resistance ($R_{SET} = 10^5 \ldots 10^6 \Omega$) and the cable capacitance ($\approx 500$ pF), constituting roughly a 10 kHz low pass. The integration time $R_2C_2$ was typically set much slower, i.e., on the order of 100 ms, to prevent the system from oscillations. The quasi dc measurements were performed by scanning one or more gates point by point, recording the signal $U_{fdbk}$ (or $U_{out}$) for typically 1 s and performing statistics and Fourier transform. The gate voltage step size could be set arbitrarily small, while the resolution was limited by thermal or vibrational noise of the signal lines ($\sim 10^{-8}$ V rms). The readout electronics for this experiment was optimized for stability rather than sensitivity or bandwidth in order to minimize external disturbances on the SET and its environment.

### C. Results

SET devices of types A and B (see Fig. 1) were systematically investigated by taking $IV$ characteristics and noise figures as a function of the four gates. The individual gate capacitances, which are listed in Table I, were consistently determined by measurement of Coulomb blockade peak spacings $\Delta U_G = e/C_G$ as well as from the feedback method using Eq. (3).

TABLE I. Gate capacitances in units of (aF) for two multigate SETs (see Fig. 1) as determined from Coulomb blockade peak spacing measurements.

| device type | G1 | G2 | G3 | G4 |
|---|---|---|---|---|
| A | 25.4 | 9.89 | 3.30 | 9.63 |
| B | 28.3 | 5.40 | 5.54 | 3.76 |

By means of the feedback circuitry the signal $U_{fdbk}$ was measured as a function of the voltages varied at one or more gates. We define the ''background charge offset signal''

$$\Delta Q_{offset} = \left( \Delta U_{fdbk} + \Delta U_i \frac{C_i}{C_{fdbk}} \right) C_{fdbk}, \tag{5}$$

where $\Delta U_i$ is the step size of the gate sweep. $Q_{rms}$ will then be denoting the rms noise on the $\Delta Q_{offset}$ signal. The data acquisition was performed by recording real-time signals at a 10-kHz sampling speed during one second, i.e., $Q_{rms}$ was measured in the bandwidth $1 \ldots 10^4$ Hz which is the relevant frequency range dominated by $1/f$ noise. The value of $\Delta Q_{offset}$ is zero when the SET electrometer is linearly modified by the gate potentials only, and shows peaks for discontinuous variations of background charges. The response of $U_{fdbk}$ and $\Delta Q_{offset}$ is schematically depicted in the inset of Fig. 3. By scanning one single gate up and down, we found nonzero $\Delta Q_{offset}$ events which reproducibly appear at the same gate voltage $U_i$ while showing hysteresis of different magnitude. The observations are consistent with former measurements on background charge fluctuations.[15] However, in Ref. 15 only a discrete resolution of the gate dependence was

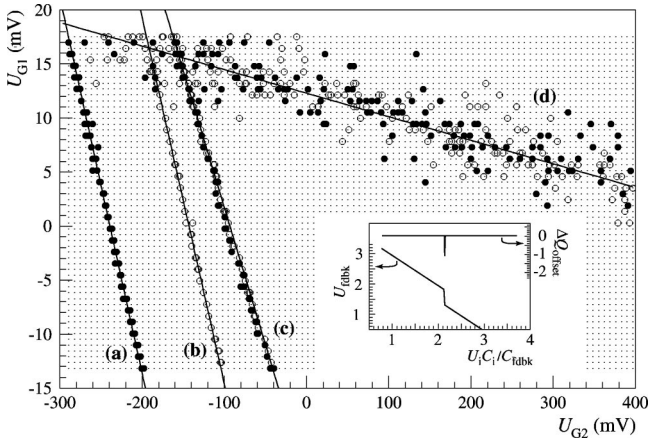


FIG. 3. Example of background charge fluctuation events with $(Q_{rms})^2 + (\Delta Q_{offset})^2 > (0.03e)^2$, due to variation of gates G2 and G1, as measured with a type A device. The straight lines are numerically fitted to the data. Circles and dots are drawn for up and down sweeps of $U_{G2}$, respectively. Only every fifth measurement point (small dots) in $U_{G2}$ is shown for clarity. The inset depicts schematically the response of $U_{fdbk}$ and $\Delta Q_{offset}$ as a function of increasing gate voltage $U_i$ with the occurrence of one trap state transition: $U_{fdbk}$ experiences a step while $\Delta Q_{offset}$ shows a peaked deviation from zero (scales in arbitrary units).

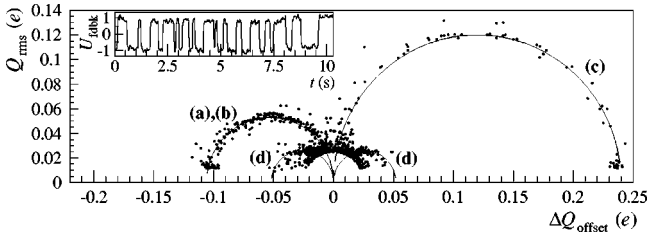


FIG. 4. Noise vs signal in units of the elementary charge $e$ plotted from data of the same measurement as in Fig. 3. The semicircles are fitted to the data points as described in the text. The intrinsic noise with $Q_{\mathrm{rms}}^2+\Delta Q_{\mathrm{offset}}^2<(0.025e)^2$ is cut off for clarity. The inset shows a $U_{\mathrm{fdbk}}$ signal (in arbitrary units) as a function of time at a transition point where increased two-level fluctuations occur.

possible via analysis of the Coulomb blockade peak positions, whereas here we are able to scan an arbitrary and continuous gate range.

#### *1. Sweeping of two gates*

If two gates are swept simultaneously (plus a third gate always acting as feedback), the local potential around the multigate SET is a strong function of the device geometry. The second gate shifts the potential threshold of a charge trap depending on its position. A measurement with two simultaneous gates swept is shown in Fig. 3. The circles and dots correspond to events from up and down sweeps of gate $G_2$, respectively, where $|\Delta Q_{\mathrm{offset}}|$ is above the instrumental and background noise. After each $G_2$ sweep, $U_{G1}$ is incremented. The events fall on different straight lines with different slopes. Depending on the linear combination of the gate voltages involved, patterns different from Fig. 3 were obtained, i.e., including positive slopes, displaying more or less scatter, showing merging event lines or sudden breaks. Measurements with all possible gate permutations on the same device were performed.

Under constant cryogenic conditions, the experimental results were highly reproducible, even after weeks. Although the noise spectrum level of our devices ($10^{-4}\ldots10^{-3}e/\sqrt{\mathrm{Hz}}$ at 10 Hz) is comparable to literature values for standard SETs,[4] we mostly observe a remarkably high long-term stability of our samples, i.e., no drift and hardly any spontaneous jumps in $IV$ characteristics. We attribute this high stability in first line to the very slow cooling of the devices (about one day with very little exchange gas), which allows the traps to equilibrate in their lowest states. However, it is empirically established that the characteristics of background fluctuations change drastically upon thermal cycling.

#### *2. Signal height*

Signal height $\Delta Q_{\mathrm{offset}}$ and rms noise $Q_{\mathrm{rms}}$ from one measurement are shown in Fig. 4, taking the same data as in Fig. 3. A clear semicircle correlation between noise and signal is observed. The lines are fits of

$$\left(|\Delta Q_{\mathrm{offset}}|-\frac{|\Delta Q_0|}{2}\right)^2+{Q_{\mathrm{rms}}}^2=\left(\frac{\Delta Q_0}{2}\right)^2 \qquad (6)$$

to the data points, where $\Delta Q_0$ is the full signal height due to one individual trap transition. This correlation suggests a perturbation based on two-level fluctuations while its observation is a consequence of the measurement system: $Q_{\mathrm{rms}}$, which is the rms value of the signal taken for 1 s, averages quadratically over possible two-level fluctuations. Assuming that the signal fluctuates during the measurement between zero and $\Delta Q_0$ where it spends the total times $t_1$ and $t_2$, respectively, and the transitions are negligibly fast, the average and the rms values of this signal would be

$$\Delta Q_{\mathrm{offset}}=\frac{t_2\Delta Q_0}{t_1+t_2},$$

$$Q_{\mathrm{rms}}=\sqrt{\frac{t_1\Delta Q_{\mathrm{offset}}^2+t_2(\Delta Q_0-\Delta Q_{\mathrm{offset}})^2}{t_1+t_2}}. \qquad (7)$$

It is easily shown that relations (7) correspond to Eq. (6). One interesting piece of information from Fig. 4 is the correspondence between the events falling on a semi-circle and those building a straight line in Fig. 3, which is represented by the labels (a)–(d). This allows to identify and correlate switching events from individual traps by both the gate dependence and the signal height.

By approaching and crossing a two-level state transition point the balance between flips and flops should, in principle, gradually change. Therefore, one might expect that the data in Fig. 4 yield detailed information on capture and escape rates of the traps involved (e.g., by observing a maximum fluctuation noise $Q_{\mathrm{rms}}$ at the transition point with a nonzero width as a function of gate voltage). However, we have found no correlation between $Q_{\mathrm{rms}}$ (or $\Delta Q_{\mathrm{offset}}$) and the position relative to the events on the lines in Fig. 3. This is apparently due to the metastability of the states where time constants are exponentially large, as discussed in Sec. III.

#### *3. Gate polarization and noise*

The noise figures of SETs are in general determined by input charge noise and the level is proportional to the SET gain.[16] However, in our case where the operation point (i.e., gain, island charge) is kept constant, eliminating the dominant noise dependence, we observe the noise level from background charge fluctuations to clearly depend on the polarization of the surrounding by variation of the gate potentials, as shown in Fig. 5.

The large fluctuations (black dots) in the upper part of Fig. 5 naturally correspond to the events drawn in the lower part where $\int\Delta Q_{\mathrm{offset}}\,\mathrm{d}U_{G1}$ experiences a step response at the transition point and $Q_{\mathrm{rms}}$ averages over the two level states. In addition, a significant abrupt change in noise is observed at $U_{G3}=73$ mV and in the range $-190\ \mathrm{mV}<U_{G1}<-170$ mV. Also, gradual variations of the noise level as a function of gate potential are measurable. While the onset of higher noise at $U_{G3}=73$ mV is observed as a unique event with increasing $U_{G3}$, the features around $U_{G1}\approx-180$ mV show an interesting combination of noise figure and trap metastability: with increasing $U_{G1}$ the trap alters its charge configuration such that the charge noise seen by the SET is

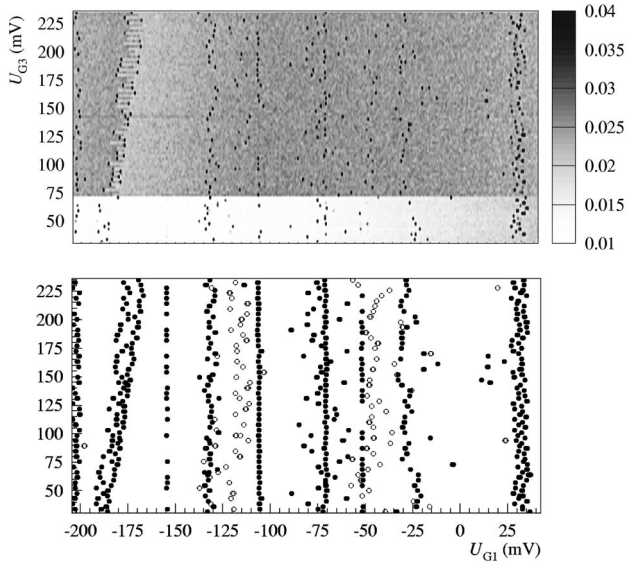


FIG. 5. Top: Gray scale plot of noise level $Q_{\mathrm{rms}}$ of the feedback signal (in units of $e$, see scale on the right) as a function of the gate voltages $U_{G1}, U_{G3}$ measured on a type B device (experimentally, $U_{G3}$ is incremented after each consecutive $U_{G1}$ scan). The data are compressed at 1/3 of the full noise spectrum to enhance visibility. Bottom: Background charge switching events for $\Delta Q_{\mathrm{offset}} > 0.2e$ (same data as above). Circles and dots are drawn for up and down gate sweeps, respectively. Signals with negative polarity are omitted for clarity.

reduced. By reversing the G1 sweep direction, the noise level is again minimal right before the trap switches back, whereas the gate voltage threshold of that transition is lower.

The transition at $U_{G3} = 73$ mV in the upper plot of Fig. 5 does not show switching events in the lower plot. This is, besides an apparent insensitivity of that trap to $U_{G1}$, an artifact of the measurement procedure: $U_{G3}$ is incremented at the end of an $U_{G1}$ sweep, therefore transitions dominated by $U_{G3}$ occur only at the turning points, i.e., the $U_{G1}$ extrema, and are not drawn in the plots.

#### *4. Superconductivity and magnetic field*

While most of the measurements have been performed with the SET in the normal state, we have also carried out test experiments in the superconducting state to investigate reproducibility. In none of the cases have we found any difference in feedback response between normal and superconducting devices. Nor did we find any indication of magnetic field dependence (for normal state SET with $B > 0.5$ T).

#### *5. No bias voltage dependence*

A further important observation is the independence of the experimental results from the biasing conditions, i.e., the source-drain voltage, neither on magnitude nor on polarity. This has been reported already in Ref. 15. The electric field within a thin tunnel junction changes drastically upon small variation of the source-drain voltage, which should yield a clearly observable effect in case of trap polarization inside the junction. In contrast, the surrounding is hardly influenced for comparable voltages ranging within the Coulomb gap (on the order of 1 mV).

#### *6. Spread of Coulomb blockade peak spacings*

Finally, it is worth noticing an interesting experimental fact we additionally discovered during measurements: when accurately determining the Coulomb blockade peak positions and calculating the nearest neighbor peak spacings $\Delta U_G$ (which are theoretically expected to be exactly $e/C_G$), we observed an increased statistical variation of $\Delta U_G$ for measurements with gates at larger distance, i.e., lower $C_G$. This is at first sight counter intuitive, because voltage noise $U_n$ (from readout electronics or noise on the cables) at the gates with lower $C_G$ should have much less effect on the SET island than nearby gates, since the image charge influenced on the island is proportional to $U_n C_G$. A possible interpretation of the results is related to the trap density of states between island and gate. The larger the number of charge fluctuators polarizable by the gate variations, the larger the statistical fluctuations sensed by the SET island. The measurements can be considered as a statistical probe of the charged environment in contrast to the experiments with discrete charge switching events. And because a larger voltage variation at more distant gates is required to modulate the SET island charge by one electron, more traps in those gate regions experience a transition, which is reflected by increased statistical (not amplitude) fluctuations.

Although the phenomenon is clearly, consistently and reproducibly observed, it is unfortunately a very small effect (a few percent) which does not permit a quantitative analysis yet. More experiments with specifically designed structures may improve resolution and allow, e.g., a determination of a trap density of states.

## III. DISCUSSION

The invariability of our results upon different biasing conditions (source-drain voltage, superconducting device) mentioned right above strongly suggests that the switching processes observed can not reside within the tunnel junctions themselves. Apart from a few exceptions in literature[5] where the results were interpreted in terms of trap fluctuations within the tunnel junction, it is generally believed that the dominant low frequency noise source is due to fluctuators located within the substrate or the oxide surrounding the SET device.[4]

Taking this into account, the simplest model to describe the process responsible for the observed charge switching events is a bistable trap,[17] located somewhere close to the SET island, where a charge can hop (or rather tunnel) between two adjacent sites back and forth.[18] This picture is equivalent to a reversible dipole. Phenomenologically the polarity of the charge is of no importance in our case and is not distinguishable either. Therefore the charge carrier involved is always taken to be an electron for simplicity. The trap configuration can change by variation of potentials (i.e., gate voltages), by thermal activation or due to PAT. The results from our experiments are clearly dominated by the po-

tential landscape intentionally modified by the four gates, although other effects may play a role at much smaller energy scales.

For illustration imagine an electron trapped in a local impurity state. An electric field, which is in our case determined by linear superposition of the potentials of the four gates and the source-island-drain structure, can force that electron to switch to a nearby metastable trap site. If the electron, e.g., shifts closer to the SET island, the latter experiences a charge reduction, which is compensated for by a signal from the feedback circuit according to Eq. (5). This explains geometrically the signal height and polarity of individual fluctuators as presented in Sec. II C 2.

The striking reproducibility of switching events as a function of the gate voltages allows detailed analysis of the traps involved. The data shown in Figs. 3 and 4 illustrate the distinct nature of individual traps. From the lines fitted to the data in Fig. 3 it was derived that the events of (a) and (b) have exactly the same slopes $dU_{G1}/dU_{G2}$, and they also show the same signal height spectrum in Fig. 4. They are only distinguished by their transition voltage threshold, which depends on gate sweep direction with a specific hysteresis of $\Delta U_{G2}=93.2$ mV in this case. According to the trapping process (charging–discharging) we like to refer to the events represented by circles and dots as flips and flops, respectively. In contrast to events (a) and (b), the transition thresholds of flips and flops on line (c) are indistinguishable, i.e., displaying a vanishing hysteresis. Yet another behavior is observed for the events on (d) which scatter very strongly. They also show both signal polarities (but of same magnitude), irrespective of gate sweep direction (see Fig. 4). This specific trap is unstable within an unusually broad gate voltage window. This is probably caused by interactions with other traps in close vicinity, rather than by pure thermal activation or PAT which we can exclude due to the large excitation energies required. In addition to the feasibility of assigning the experimental data as shown in Figs. 3 and 4 to individual traps, we can also make an identification by relating the flip and flop thresholds of the same trap from an experiment as presented in Fig. 6.

The measurement in Fig. 6, where the gate voltage range is increased with each consecutive sweep, clearly shows that a trap can only switch off (flop) if it has also been switched on (flip) before, or vice versa. This is consistent with and suggestive of the single charging nature of the traps observed here.

Although some events in Fig. 6 are detected at the same threshold, i.e., the flops of (b) and (c) or the (a) flips and the (d) flops, we can again easily identify them due to clear distinction in the noise vs signal height diagram (like in Fig. 4, but not shown in this case).

The behavior of the traps in general seems to be only very weakly influenced by other fluctuators. This is concluded from the straight lines found in measurements like in Figs. 3 or 6. The transition threshold is usually not altered irrespective of the polarization strength of the environment (Fig. 6), i.e., there is no difference whether a small or a large gate potential was applied, the trap switching occurs at the same gate voltages. A rarely clear exception is seen in the events

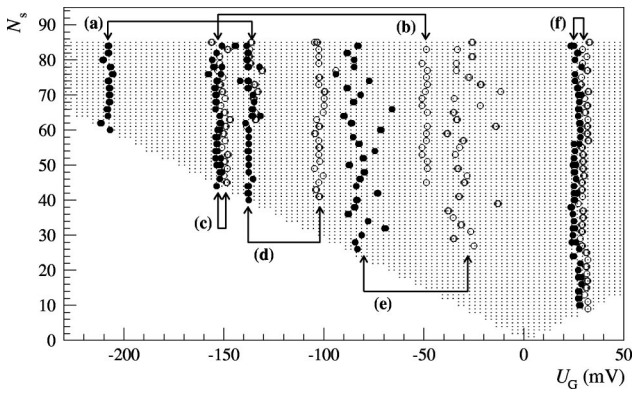


FIG. 6. Charge fluctuations with $\Delta Q_{\text{offset}} \geqslant 0.02e$ measured with a type B device by increasing the gate scan range with increasing scan number $N_s$ (only a selected part of the entire measurement is shown). Events with negative $\Delta Q_{\text{offset}}$ polarity show similar correlations, but they are omitted for clarity. The flip and flop thresholds according to transitions of one individual trap can be related by their onset and are denoted by arrows. The small dots (grid) represent every fifth measurement point in $U_G$.

(f) in Fig. 6, which show slight shifts at the onsets of traps (a) and (e), i.e., for $N_s=60$ and 26, respectively. This suggests a rather small distance of these particular traps among each other allowing electrostatic interaction. In general, however, according to simple electrostatics, charges (or traps) in very close vicinity to metallic electrodes are strongly screened.[19] The suppressed interaction leads to the observation of individual unperturbed charge trapping events.

From the characteristics of individual traps, i.e., their transition thresholds as a function of polarization of their environment, we cannot only distinguish but also localize the fluctuators. Variation of two gates electrostatically determines the equipotential line where the trap switching occurs. The relation of the gate potentials is extracted from the slope $dU_{Gi}/dU_{Gj}$ of an individual trap as taken e.g., from Fig. 3. Addition of more gates simply modifies the linear combination of electric potentials involved, allowing to verify the results from experiment and calculations. The exact position (and size) of the trap relative to the SET island is then determined by the signal height and polarity. An estimate for charge variations on the island on the order of $0.1e$ shows that the observable traps (with a typical extension of $\approx 2$ nm) must reside in the very close vicinity of the island.[15]

We have performed numerical electrostatics calculation (equipotential lines) on the device, based on a quasi-threedimensional finite element method (real two-dimensional finite element calculations in the substrate plane with iterative corrections in the third dimension). An example of a potential calculation for the trap events (a) and (b) of Fig. 3 is shown in Fig. 7. Gates G3, G4, and the source-island-drain line are at zero potential while gates G1 and G2 are at relative potentials defined by the slope $dU_{G1}/dU_{G2}$ of Figs. 7(a) and 7(b). This yields an equipotential line for zero variation labeled (a) and (b). The white dot [on the lower right edge of the island, also labeled (a) and (b)] finally represents the location of that particular trap. Calculated equipotential lines are also drawn for trap events (c) and (d),

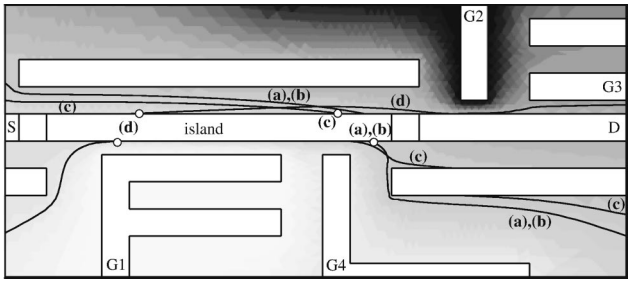


FIG. 7. The potential landscape (gray scale) is shown for the slopes [(a) and (b)] from Fig. 3. Calculated equipotential lines for zero variation are drawn for all slopes from that experiment. The white dots at the edge of the island mark the positions of the fluctuators. Accuracy of the calculated position tangential to the island is numerically estimated to be about 10 nm. The perpendicular position is given by the signal height and limited to a few nanometers.

respectively. The trap location (d) is ambiguous and drawn on both island sides due to not well defined signal polarity (see Fig. 4).[23]

This feature to determine the position of individual traps while studying their specific behavior opens up a new method to study the substrate, surface, interface or oxide quality which are of increasing importance in nanostructure devices. Of course, the method is limited by the ability to observe distinct finite slopes in $dU_{Gi}/dU_{Gj}$. The majority of the data in Fig. 5 is therefore not useful for trap position determination. The data simply reflects a negligible influence of gate G3 on the measured traps due to screening by other gates in our structure not specifically intended for such experiments. The problem can easily be resolved by optimized and more sophisticated lithographic design (e.g., a starlike arrangement of gates to minimize electrostatic screening between traps and SET island).

On the other hand we wish to emphasize the possibility to optimize the operation point of a real device like an electron pump or a turnstile by noise analysis as shown in Sec. II C 3. The stable operation of SET devices with respect to background charge fluctuations is one of the biggest issues in their implementation into useful circuits. With an appropriate device structure and the method described here we can find the working point of optimum signal to noise ratio or maximize device stability, as required for low noise applications.

The origin of hysteresis as observed in our experiments is a rather delicate problem and not fully understood. In general, hysteresis or metastability may be due to asymmetric tunnel barriers, to polarization of the proximal environment (including other traps), or to multiple tunneling processes.[20] We are not able to decide on the dominant microscopic origin of the hysteresis measured in our case. However, our observation of increased fluctuations close to a transition point indicates that there are different energy scales and more than one single mechanism involved. The time constants of the generation-recombination processes[21] are unfortunately, due to hysteresis, either astronomically large or at scales which are not accessible with our experimental setup (readout electronics bandwidth $<10$ kHz). The spectrum of hysteresis values (energy difference between flip and flop) was found to be flat up to several 100 mV (i.e., covering the entire gate sweep range). This prevents us from extracting quantitative data on the metastability of the traps which apparently have an average energy spread much larger than is accessibly with our method. This is also related to the fact that we do not observe periodic multiple charging of the same trap. Probably the trap size and the equivalent capacity are so small that the charging energy can be far above 1 eV.

Nevertheless, we can make a very rough estimate of the trap density assuming that all the observed fluctuators reside on the island surface (i.e., traps in the oxide covering the island). The island surface facing the gate (i.e., perpendicular to the electric field) has an area of $60\times1000$ nm$^2$. We measure an extrapolated average of 20 traps per volt of gate variation. That yields an interface (or surface) trap density of roughly $3\times10^{10}$ eV$^{-1}$ cm$^{-2}$. We believe this is quite a reasonable number and it is well consistent with literature values[1] (although those are given for silicon, the order of magnitude should be applicable).

As a final remark, we wish to comment on one possible origin of the charge traps responsible for the switching events. Empirically we have observed significantly less fluctuators in a 'fresh' device at the very first cool-down compared to measurements after thermal cycling. This may suggest that the imperfections are (also) a consequence of mechanical stress. The effect of electrical stress on noise characteristics has been reported in Ref. 22.

## IV. CONCLUSION

We have presented an experimental method and measurement results on electrometric performance of a modified single–electron device. The technique allowed us to study charge traps individually, exploring the very fluctuators which are responsible for noise and instabilities, severely degrading the operation of mesoscopic electronic devices. In particular, the charge background was investigated by scanning different gates simultaneously and recording abrupt changes of the SET island polarization. The experimental results were highly reproducible and therefore allowed extensive systematic studies. We were able to distinguish switching processes due to individual charge traps. The knowledge of trap transition threshold and signal height allowed to geometrically determine the trap position, which was typically not more than a few nanometers away from the island surface. The tangential accuracy of the analysis was estimated to be about 10 nm. This provides an alternative method to, e.g., scanning imaging experiments[7] for local investigation of trapping processes.

The noise level of the SET device was found to depend on the environment polarization due to gate potential variations. The reproducible experiments offer a method to determine the noise characteristics of the SET and to adjust the operation point for maximum signal to noise or best device stability. It is particularly advantageous that the testing of the charge background is performed with the same working device, i.e., the optimization detector and subsequent application device are the same.

The fluctuators observed in the experiments are exclusively located in the close vicinity of the SET island, i.e., in the oxide covering the island or in the substrate. In the former case we have roughly estimated a trap density of $3\times10^{10}$ eV$^{-1}$ cm$^{-2}$, which compares very well with literature values.

**ACKNOWLEDGMENTS**

We are grateful to Klaus Ensslin, Alexander B. Zorin, Blaise Jeanneret, Beat Jeckelmann, and Felix Meli for valuable discussions and support. This work was supported in part by the EU (Project COUNT).

*Present address: Laboratory for Astrophysics, Paul Scherrer Institute, CH-5232 Villigen PSI, Switzerland.

[1] E. Simoen and C. Claeys, Solid-State Electron. **43**, 865 (1999).

[2] D. V. Averin and K. K. Likharev, in *Mesoscopic Phenomena in Solids*, edited by B. A. Altshuler, P. A. Lee, and R. A. Webb (Elsevier, Amsterdam, 1991), pp. 173–271; *Single Charge Tunneling: Coulomb Blockade Phenomena in Nanostructures*, Vol. 294 of *NATO Advanced Study Institute, Series B: Physics* edited by H. Grabert and M. H. Devoret (Plenum, New York, 1992).

[3] T. A. Fulton and G. J. Dolan, Phys. Rev. Lett. **59**, 109 (1987).

[4] G. Zimmerli, T. M. Eiles, R. L. Kautz, and J. M. Martinis, Appl. Phys. Lett. **61**, 237 (1992); A. B. Zorin, F.-J. Ahlers, J. Niemeyer, T. Weimann, H. Wolf, V. A. Krupenin, and S. V. Lotkhov, Phys. Rev. B **53**, 13 682 (1996); N. M. Zimmerman, J. L. Cobb, and A. F. Clark, *ibid.* **56**, 7675 (1997); A. N. Tavkhelidze and J. Mygind, J. Appl. Phys. **83**, 310 (1998); V. A. Krupenin, D. E. Presnov, M. N. Savvateev, H. Scherer, A. B. Zorin, and J. Niemeyer, *ibid.* **84**, 3212 (1998); D. E. Grupp, T. Zhang, G. J. Dolan, and N. S. Wingreen, Phys. Rev. Lett. **87**, 186805 (2001).

[5] D. Song, A. Amar, C. J. Lobb, and F. C. Wellstood, IEEE Trans. Appl. Supercond. **5**, 3085 (1995); M. Kenyon, J. L. Cobb, A. Amar, D. Song, N. M. Zimmerman, C. J. Lobb, and F. C. Wellstood, J. Low Temp. Phys. **123**, 103 (2001).

[6] K. S. Ralls, W. J. Skocpol, L. D. Jackel, R. E. Howard, L. A. Fetter, R. W. Epworth, and D. M. Tennant, Phys. Rev. Lett. **52**, 228 (1984): D. H. Cobden, N. K. Patel, M. Pepper, D. A. Ritchie, J. E. F. Frost, and G. A. C. Jones, Phys. Rev. B **44**, 1938 (1991); T. Sakamoto and K. Nakamura, Superlattices Microstruct. **23**, 413 (1998); M. G. Peters, J. I. Dijkhuis, and L. W. Molenkamp, J. Appl. Phys. **86**, 1523 (1999).

[7] M. E. Welland and R. H. Koch, Appl. Phys. Lett. **48**, 724 (1986); R. Crook, C. G. Smith, M. Y. Simmons, and D. A. Ritchie, J. Phys.: Condens. Matter **13**, L249 (2001).

[8] R. J. Schoelkopf, P. Wahlgren, A. A. Kozhevnikov, P. Delsing, and D. E. Prober, Science (Washington, DC, U.S.) **280**, 1238 (1998).

[9] V. A. Krupenin, D. E. Presnov, A. B. Zorin, and J. Niemeyer, J. Low Temp. Phys. **118**, 287 (2000).

[10] R. L. Kautz, M. W. Keller, and J. M. Martinis, Phys. Rev. B **62**, 15 888 (2000).

[11] K. Yano, T. Ishii, T. Hashimoto, T. Kobayashi, F. Murai, and K. Seki, IEEE Trans. Electron Devices **41**, 1628 (1994).

[12] J. Niemeyer, PTB-Mitt. **84**, 251 (1974); G. J. Dolan, Appl. Phys. Lett. **31**, 337 (1977).

[13] M. Furlan and B. Jeanneret, OFMETInfo **6/2**, 3 (1999).

[14] A. B. Zorin, Rev. Sci. Instrum. **66**, 4296 (1995).

[15] M. Furlan, T. Heinzel, B. Jeanneret, S. V. Lotkhov, and K. Ensslin, Europhys. Lett. **49**, 369 (2000); M. Furlan, T. Heinzel, B. Jeanneret, and S. V. Lotkhov, J. Low Temp. Phys. **118**, 297 (2000).

[16] B. Starmark, T. Henning, T. Claeson, P. Delsing, and A. N. Korotkov, J. Appl. Phys. **86**, 2132 (1999).

[17] For reviews, see e.g.: M. J. Kirton and M. J. Uren, Adv. Phys. **38**, 367 (1989); Sh. Kogan, *Electronic Noise and Fluctuations in Solids* (Cambridge University Press, Cambridge, 1996).

[18] H.–O. Müller, M. Furlan, T. Heinzel, and K. Ensslin, Europhys. Lett. **55**, 253 (2000).

[19] M. Schulz, Microelectron. Eng. **40**, 113 (1998).

[20] P. D. Dresselhaus, L. Ji, Siyuan Han, J. E. Lukens, and K. K. Likharev, Phys. Rev. Lett. **72**, 3226 (1994).

[21] R. N. Hall, Phys. Rev. **87**, 387 (1952); W. Shockley and W. T. Read, *ibid.* **87**, 835 (1952).

[22] D. H. Cobden, M. J. Uren, and M. Pepper, Phys. Rev. Lett. **71**, 4230 (1993).

[23] Note that the equipotential lines seem to cross the island, which of course is not possible with a metallic island in two dimensions. However, keep in mind that Fig. 7 shows a three dimensional projection on the two-dimensional plane (or a cut of equipotential surfaces). The lines are effectively neither touching nor crossing the metal. The trap positions are determined where the lines approach the island at a distance of $\sim$2 nm.